Antiferromagnetism and spin density waves in three-dimensional Dirac metals

Grigory Bednik
Physics Department, University of California Santa Cruz, 95064 California, USA

(Received 23 July 2019; accepted 9 April 2020; published 14 September 2020)

We study possible magnetic instabilities in Dirac semimetals. We find that Dirac electrons naturally host antiferromagnetic or spin-density wave ground states, though their specific configurations may vary depending on a specific model, as well as chemical potential and temperature. We also discuss paramagnetic susceptibility of Dirac semimetals. In the cases when Dirac electrons do not have orbital momentum, the magnetic properties may be μ and T independent.

DOI: 10.1103/PhysRevB.102.125119

I. INTRODUCTION

Weyl and Dirac semimetals (see Ref. [1] for a review) have attracted significant attention during the last years. Both of them are prominent for their band structure having effectively gapless excitations described by Weyl and Dirac equations. In the former case, their spectrum contains two nondegenerate bands, and in the latter case their two bands are doubly degenerate. Because of that, Weyl semimetals are realized when either time-reversal or inversion symmetry is broken, whereas Dirac semimetals are realized in the presence of both of them.

It is known that Weyl points in Weyl semimetals [2–8] can be viewed as monopoles of Berry curvature [9], which makes them topologically stable. Weyl points cannot be gapped under any local perturbations. The only way to destroy them is via annihilation, which can happen after moving two Weyl points of opposite charges together. In contrast, in Dirac semimetals, the Dirac points are not protected topologically. In type-I Dirac semimetals [10–15] (two experimentally discovered examples are Na_3Bi and Cd_3As_2), there are two Dirac points located opposite to each other on the z axis, which are protected by crystal rotational symmetry relative to the z axis. At the same time, in type-II Dirac semimetal $ZrTe_5$ [16,17] there is a single Dirac point at the center of the Brillouin zone, which is not protected at all: in fact the Dirac point is gapped, but the gap can be neglected because, accidentally, it is very small.

Dirac semimetals necessarily possess time-reversal and inversion symmetries, which ensure double degeneracy of their bands. Breaking one of these symmetries may lift the degeneracy, thus splitting the Dirac point into a pair of Weyl points. It can also lead to more complicated combinations of Weyl points and rings [4,18]. The most natural way to achieve it is to add an intrinsic Zeeman field into the system. The behavior of Dirac semimetals under extrinsic magnetic fields applied in specific directions has been extensively studied, and, for instance, it was found that, in the simplest model of $ZrTe_5$, the Dirac point can split into two Weyl points, if the Zeeman field is applied in the z direction, or into a nodal ring if the Zeeman field is applied in the xy plane [19].

However, it is not yet fully understood whether magnetization in Dirac semimetals may happen spontaneously. Recently, magnetic properties of Dirac electrons interacting with magnetic impurities have been studied [20–23]. Magnetic impurities are known to obey the Ruderman-Kittel-Kasuya-Yosida interaction, which has complicated oscillating and anisotropic structure and thus does not make it possible to find the resulting magnetic ground state. In the works [24–26], magnetic susceptibility of Dirac semimetals at small external magnetic fields was studied, and a few remarkable properties were found. In particular, it was found that the susceptibility in Dirac semimetals is determined not only by the Fermi surface, but by the whole Brillouin zone, and moreover it may be independent of the Fermi energy, but dependent on the boundary properties of the Brillouin zone.

Magnetic instabilities have also been studied in various systems, similar to Dirac semimetals, such as three-dimensional (3D) Fermi gas with Weyl-like spin-orbit coupling [27], Dirac electrons on a surface of a topological insulator [28–33], and particularly Weyl semimetals [34–39]. It was found that in these systems various phases can emerge, including spin-density waves [27,29,34].

On the other hand, in the recent years a large number of antiferromagnetic Dirac semimetals have been discovered experimentally, which include CuMnAs [40–43], $CaMnBi_2$ and $SrMnBi_2$ [44,45], NdSb [46–49], and $EuCd_2As_2$ [50]. These materials are currently widely explored in the context of possible spintronics applications [43,51–53] (see Ref. [54] for a review). However, their electronic structure is rather complicated and includes both localized and conduction electrons. Their phase diagrams are also nontrivial.

Motivated by this knowledge, we study a simple problem of spontaneous magnetization in 3D Dirac semimetals (which can arise either due to magnetic impurities or due to interactions) using mean-field approximation [55,56]. A similar approach was previously used to find preferred magnetic states in semiconductors with quadratic band touching [57,58]. We find that 3D Dirac semimetals may host antiferromagnetic or spin-density wave ground states, depending on their Fermi level. We observe transitions between different magnetic ground states as functions of Fermi energy and temperature.

Specifically, we consider two most commonly used models of 3D Dirac semimetals: a model describing type-II Dirac semimetal $ZrTe_5$ with one Dirac point at the center of the Brillouin zone, and a model describing type-I Dirac semimetal Na_3Bi with two Dirac points separated in momentum space. We introduce magnetization fields in these models (which may have finite momentum corresponding to spatial modulation of the magnetization), compute their effective actions up to quadratic order, and thus demonstrate that the magnetic instabilities are spatially modulated. After this, we place these models on a lattice and compute the effective actions for magnetization numerically. In this way, we are able to see at which momentum the effective actions reach a minimum, i.e., when magnetizations become stable. We obtain that at small chemical potentials the minimum of the effective action is reached at the boundary of the Brillouin zone, which implies that the magnetic ground states are antiferromagnetic. On the other hand, as the chemical potential increases, the minimum of the effective action shifts away from the boundary of the Brillouin zone, and thus the magnetic ground state changes into an incommensurate spin-density wave. Eventually, there may happen a transition into a ferromagnetic ground state.

In addition, we compute the effective actions at finite temperature. We obtain their analytical expression for the case of zero external momentum, which provides us knowledge about paramagnetic susceptibility of the Dirac semimetals. We find that, typically, the paramagnetic susceptibility decreases $\propto T^2$. However, in certain cases, particularly when Dirac electrons do not have orbital momentum, the susceptibility may be μ and T independent. Finally, we compute the effective action numerically at finite temperatures and see that the wave vector of the spin-density wave changes as a function of temperature. This leads us to the conclusion that there may exist transition between commensurate antiferromagnetic and incommensurate spin-density wave ground states as a function of temperature.

This paper is organized as follows. In Sec. II, we compute the effective actions for both our models analytically at zero temperature. In particular, in Sec. II A we focus on the case of a Dirac semimetal with one Dirac point (i.e., type II), and in Sec. II B we consider a Dirac semimetal with two spatially separated Dirac points (i.e., type I). In Sec. III, we compute paramagnetic susceptibility at finite temperatures for both type-II and -I Dirac semimetals. We summarize our findings and their possible implications in Sec. IV. Finally we present our numerical results in the Appendix.

II. SPONTANEOUS MAGNETIZATION AT ZERO TEMPERATURE

In this section we study spontaneous magnetization in two simple models of type-II and -I Dirac semimetals. Specifically, we introduce the magnetization field, compute its effective action up to the second order over the field and its momentum, and use it to find possible magnetic instabilities. We start from the simplest model of a type-II Dirac semimetal containing a single Dirac point and use it to illustrate our method. After this, we repeat the calculations in the case of the slightly more complicated model of a type-I Dirac semimetal, which contains a pair of Dirac points separated in momentum space.

A. Type-II Dirac semimetal

Here we analyze the model of a type-II Dirac semimetal, which has a single Dirac point at the center of the Brillouin zone. We note that an experimental example of such a Dirac semimetal is $ZrTe_5$. Its band structure is invariant under time-reversal symmetry, inversion symmetry, and three mirror symmetries. The Hamiltonian [16] can be written as

$$H_0 = \sum_{k,i} d_i(k)\Gamma_i, \tag{1}$$

where Γ_i are five gamma matrices defined as tensor products of Pauli matrices σ and τ acting in spin and pseudospin spaces, namely,

$$\Gamma_1 = -\tau_z\sigma_z, \qquad \Gamma_2 = \tau_y, \qquad \Gamma_3 = \tau_z\sigma_x,$$
$$\Gamma_4 = -\tau_z\sigma_y, \qquad \Gamma_5 = -\tau_x.$$

The coefficients d_i have, in general, a complicated form determined by the whole structure of the Brillouin zone, but near the Dirac point they can be approximated as linear functions of momentum:

$$d_1 = 0, \qquad d_2 = v_z k_z, \qquad d_3 = v_y k_y,$$
$$d_4 = v_x k_x, \qquad d_5 = m \approx 0. \tag{2}$$

Here $v_{x,y,z}$ are Fermi velocities in all possible directions, which, in general, may be different, since the crystal structure is anisotropic, and m is a gap in the Dirac point, which, strictly speaking, exists but can be neglected because it is very small.

In a conventional way (see, e.g., Ref. [55]), we introduce magnetization by adding to the Hamiltonian an interaction term:

$$H_1 = U \int dx(\psi^+ S\psi)^2. \tag{3}$$

We emphasize that since electrons in $ZrTe_5$ have spin, but do not have an angular momentum, S is just an electron spin, which has a simple expression $S_i = \frac{\sigma_i}{2}$.

After performing Hubbard-Stratonovich transformation, it is possible to get rid of the quartic term (3) by introducing magnetization field $M(q)$, which is just a superposition of spin matrices: $M(q) = \sum_i b_i(q)S_i$. Thus the total Hamiltonian of our system takes the form

$$H = H_0 + \frac{U}{4}\sum_q M^2 - \frac{U}{2}\sum_{k,q} \psi^+(k+q)M(q)\psi(k), \tag{4}$$

which is just a sum of a free-fermion Hamiltonian, the kinetic term for the magnetization field, and the Zeeman interaction between them. We note that the magnetization field is assumed to have a finite momentum q, which corresponds to its spatial modulation.

The effective action for the magnetization field is obtained by writing the partition function for a system with the total Hamiltonian (4) as a path integral and integrating the fermions out. The leading correction to the magnetization kinetic term M^2 can be written in terms of the fermionic Green's function

$G(w,k)=[iw-H_0(k)]^{-1}$ as

$$S=\frac{1}{\beta}\sum_{w,k,q}\mathrm{tr}G(w,k)M(-q)G(w,k+q)M(q). \tag{5}$$

Here, k is an internal momentum, and q is the external momentum, corresponding to the spatial modulation of the magnetization. We note that, in this section, we are primarily interested in a possible spontaneous magnetization, but, strictly speaking, the same Eq. (5) describes momentum-dependent spin susceptibility $\chi_{ij}(q)=-\frac{\partial^2\delta S_2}{\partial b_i\partial b_j}$.

After using the explicit expressions for M and G, performing Matsubara summation, and taking the limit of zero external Matsubara frequency, Eq. (5) takes the form

$$\begin{aligned}S=\sum_k\Bigg\{&\frac{\mathrm{tr}M^2}{2(d_+^2-d_-^2)}[d_+n_F(d_+-\mu)-d_+n_F(-d_+-\mu)-d_-n_F(d_--\mu)+d_-n_F(-d_--\mu)]\\&+\frac{\mathrm{tr}(d_+\Gamma)M(d_-\Gamma)M}{2(d_+^2-d_-^2)}\left[\frac{n_F(d_+-\mu)}{d_+}-\frac{n_F(-d_+-\mu)}{d_+}-\frac{n_F(d_--\mu)}{d_-}+\frac{n_F(-d_--\mu)}{d_-}\right]\Bigg\},\end{aligned} \tag{6}$$

where for shortness we have introduced $d_\pm=d(k\pm\frac{q}{2})$.

We proceed further by expanding Eq. (6) in powers of the external momentum q. More specifically, we have to expand $d_\pm$ and $n_F(d_\pm-\mu)$, $n_F(-d_\pm-\mu)$ in powers of q. As a result, the effective action (6) becomes rewritten as a sum of the contributions proportional to $n_F(\pm d-\mu)$ and its derivatives $\frac{\partial^m n_F(\pm d-\mu)}{\partial^m d}$, respectively. The former contribution can be viewed as a momentum k summation over all filled states and thus labeled as interband, whereas the latter can be viewed as a summation over states at the Fermi surface and thus labeled as intraband. We note that the fact that magnetization contains the contribution from outside of the Fermi surface is a special property of Dirac semimetals. We explain this peculiarity by the fact that, in Dirac semimetals, different bands approach very closely each other near the Dirac points, which is in contrast to conventional metals, where a band containing the Fermi surface is assumed to be well separated from the others.

Now let us write explicitly the terms, which appear after we expand the effective action (6) up to the zeroth order over the external momentum q. Since at zero temperature the derivative of Fermi distribution is just a minus delta function, $\frac{\partial n_F(d-\mu)}{\partial d}=-\delta(d-\mu)$, we can remove the momentum integral in the intraband contribution and thus write the effective action as

$$\begin{aligned}S^{(0)}=&\frac{1}{2\pi^2v_xv_yv_z}\int dk\left\{-\frac{2kb_\perp^2}{3}-\frac{4kb_z^2}{3}\right\}\theta(k-\mu)\\&+\frac{1}{2\pi^2}\left\{-\frac{4\mu^2b_\perp^2}{3}-\frac{2\mu^2b_z^2}{3}\right\}.\end{aligned} \tag{7}$$

Interestingly, we find that the "bulk" contribution to the effective action is divergent at large k. However, this divergence is resolved very easily: we were assuming that the dispersion is linear everywhere and unlimited, whereas in a real material the range of momenta is limited by the size of the Brillouin zone, and furthermore the dispersion becomes nonlinear far away from the Dirac point. Thus, we can view the integral entering Eq. (7) as large, but finite, and limited by nonlinearities in d and the size of the Brillouin zone. We can also track evolution of the effective action $S^{(0)}$ with change of chemical potential μ. When the Fermi level is aligned with the Dirac points, i.e., at $\mu=0$, the effective action, and consequently the magnetic susceptibility, is solely determined by the bulk of the Brillouin zone. In this special case, the z component of the magnetic field enters with the coefficient of larger magnitude, than $b_\perp$, and thus we can infer that magnetic susceptibility in the z direction χ_{zz} is larger than in the perpendicular direction (e.g., χ_{xx}).

However, the contribution to $S^{(0)}$ from the Fermi surface "competes" against the contribution from the bulk. Indeed, the Fermi surface gives larger contribution to the perpendicular component of the susceptibility than to its zz component. Thus, at sufficiently large Fermi energies, it is possible that the contribution from the Fermi surface is larger than from the bulk of the Brillouin zone, and, as a result, the susceptibility in the perpendicular direction is larger than along the z axis, oppositely to the case of small Fermi energy.

It is of interest to compute the change of effective action over the chemical potential explicitly. In the approximation of linear dispersion, it has the following expression:

$$\Delta S^{(0)}|_0^\mu=-\frac{\mu^2b_\perp^2}{2\pi^2v_xv_yv_z}.$$

This equation tells us that the variation of the effective action due to finite chemical potential depends only on the perpendicular component of the magnetic field. In other words, in the range of parameters, where the dispersion can be viewed as linear, the susceptibility in the z direction does not depend on the chemical potential. We remark that independence of observables on chemical potential is a common property of topological semimetals: the fact that susceptibility in Dirac semimetals does not depend on chemical potential is similar to the existence of universal value for anomalous Hall conductivity in Weyl semimetals, which is independent not only of chemical potential, but even of the presence of superconductivity [59,60].

In order to study possible spatial modulation of the magnetic ground state, we expand the effective action (6) up to quadratic order over external momentum q. More specifically, after we expand the terms $d_\pm$, $n_F(d_\pm)$ and its derivatives and use an identity $\frac{\partial^m n_F(d-\mu)}{\partial^m d}=-\frac{\partial^{m-1}}{\partial^{m-1}d}\delta(d-\mu)$, we obtain the

following expression for the quadratic terms in momentum:

$$S^{(2)} = \frac{1}{2\pi^2 v_x v_y v_z}\int \frac{dk}{k}\left\{-\frac{q_z^2 b_\perp^2}{6}+\frac{q_\perp^2 b_z^2}{3}\right.$$
$$\left.+\frac{(q_x b_x+q_y b_y)^2}{6}-\frac{(q_x b_y-q_y b_x)^2}{6}\right\}\theta(k-\mu)$$
$$+\frac{1}{2\pi^2 v_x v_y v_z}\left\{-\frac{q_\perp^2 b_\perp^2}{180}+\frac{43 q_z^2 b_\perp^2}{180}-\frac{19 q_\perp^2 b_z^2}{90}+\frac{q_z^2 b_z^2}{30}\right.$$
$$\left.-\frac{11(q_x b_x+q_y b_y)^2}{90}+\frac{11(q_x b_y-q_y b_x)^2}{90}\right\}. \quad (8)$$

Similarly to Eq. (7), this equation has two contributions from the bulk of the Brillouin zone and from the Fermi surface, respectively. They contain terms entering with opposite signs, which implies that the bulk and the Fermi surface compete against each other, and as a result there exists a possibility of crossovers between different phases at different Fermi energies. Specifically, at small Fermi energies, the bulk contribution dominates, since the momentum integral in Eq. (8) is determined by the UV cutoff of the Brillouin zone. However, this contribution decreases with increasing μ, whereas the Fermi-surface contribution does not depend on the Fermi level μ and thus, at sufficiently large μ, can become dominant.

Now, let us discuss the form of possible magnetic configurations. First, we consider the magnetic instability in the z direction. At small Fermi energies, the magnetic field component b_z enters the effective action with positive coefficient in front of the momentum, which implies that the magnetization in the z direction is spatially independent. We note, however, that this is due to the fact that the bulk contribution does not have a term $q_z^2 b_z^2$, which in turn happens due to linear dispersion. In principle, nonlinear corrections to $d(k)$ can lead to nontrivial bulk term $q_z^2 b_z^2$, which in turn may change the ground state into a spin-density wave modulated in the z direction, as we will see in numerical calculations.

In addition, at sufficiently large Fermi energy, the term $q_\perp^2 b_z^2$ may acquire negative coefficient, which means that magnetic field b_z will be spatially modulated in the perpendicular direction.

In a similar way, if we look at the instability in perpendicular direction $b_\perp$, Eq. (8) tells us that, at small Fermi energy, it will be spatially modulated in the transverse direction, since the effective action has negative momentum components in the z direction and in the xy plane perpendicular to the magnetization. If the Fermi level is increased, its momentum may change: the q_z component may disappear, and, furthermore, it may change from transverse to longitudinal, i.e., the momentum vector may become aligned with the magnetization direction.

Thus, we have found that the effective action for magnetization in a type-II Dirac semimetal does not reach its local minimum at zero external momentum q. This fact tells us that the magnetic state of the type-II Dirac semimetal is spatially modulated, and its preferred configuration is determined by the competition between the bulk (i.e., interband) and the Fermi-surface (i.e., intraband) contributions to the effective action. As a result, the magnetic ground state may change as the Fermi level changes. Since we are able to compute analytically the effective action only in the limit of small momenta q, we cannot obtain an explicit answer for a wavelength of the spatial modulation. For this reason, in the Appendix A 1 we compute the effective action (6) numerically at arbitrary values of the external momentum q and obtain that at small Fermi level its minimum is reached at the boundary of the Brillouin zone, i.e., when one of the components of q is equal to $\pm\pi$ (see Fig. 1). However, when the Fermi level becomes sufficiently large and nonlinear corrections to the Hamiltonian (1) become important, the minimum shifts away from the boundary of the Brillouin zone. Thus, we claim that at small Fermi level our model of a Dirac semimetal has an antiferromagnetic ground state, but as the Fermi level increases it undergoes phase transition to an incommensurate spin-density wave ground state.

B. Type-I Dirac semimetal

A type-I Dirac semimetal has two experimentally discovered examples: Na_3Bi and Cd_3As_2. It possesses a pair of Dirac points separated in momentum space in the z direction and protected by discrete rotational symmetry. We write the simplest Hamiltonian describing such a system as

$$H_0 = \sum_{k,i} d_i(k)\Gamma_i, \quad (9)$$

and, to be consistent with the previous literature [18], we define the Γ matrices in terms of Pauli matrices σ and τ as

$$\Gamma_1 = \tau_z\sigma_x, \quad \Gamma_2 = \tau_z\sigma_y, \quad \Gamma_3 = \tau_z\sigma_z,$$
$$\Gamma_4 = \tau_x, \quad \Gamma_5 = \tau_y.$$

We take the simplest possible form of the coefficients d_i:

$$d_1 = v_F k_x, \quad d_2 = v_F k_y, \quad d_3 = m(k_z),$$
$$d_4 = d_5 = 0.$$

Here $m(k)$ is a function that changes sign at two symmetric points separated in the z direction, which are indeed the Dirac points. We assume that m is positive between the Dirac points (e.g., at $k = 0$) and negative away from them.

In type-I Dirac semimetal, the Dirac points are protected by discrete rotational symmetry [61] along the z axis. Namely, states in the valence and conduction bands have different rotation eigenvalues, which makes it impossible to write a rotationally invariant term, that would gap them out. This, in turn, results from the fact that, in type-I Dirac semimetals, the valence and conduction band belong to different multiplets: the valence band is a singlet with total spin $J = 1/2$, whereas the conduction band is part of the triplet with total spin $J = 3/2$ (see, e.g., Refs. [11,18] for more details). The other bands from the triplet are separated by an energy gap, so we neglect them. Thus we start our analysis from writing a Hamiltonian of the form (4) with H_0 describing free electrons in type-I Dirac semimetals [see Eq. (9)], but we write the magnetization operator as a sum of singlet and triplet contributions

$$M = M_s + M_p,$$

which have matrix structure following from the total angular momentum of the states in the bands, namely,

$$M_s = \frac{g_s}{2}\begin{pmatrix} 0 & 0 & 0 & 0 \\ 0 & b_z & b_- & 0 \\ 0 & b_+ & -b_z & 0 \\ 0 & 0 & 0 & 0 \end{pmatrix}$$

and

$$M_p = \frac{3g_p}{2}\begin{pmatrix} b_z & 0 & 0 & 0 \\ 0 & 0 & 0 & 0 \\ 0 & 0 & 0 & 0 \\ 0 & 0 & 0 & -b_z \end{pmatrix}.$$

We note that we include in the triplet contribution only the z component of the magnetization field. This is because interaction with $b_{x,y}$ can occur only through mixing of the different bands within the triplet, which are separated by an energy gap, but we are interested in scales smaller than the width of each band. We also note that, since the conduction and valence band belong to different multiplets, they have, generically, different gyromagnetic factors, which we denote by $g_{s,p}$, respectively.

We can compute the effective action (5) in the same way, as in Sec. II A. More specifically, we can still use its expression (6) and after explicitly evaluating the traces we obtain that, at zero external momentum q, it can also be represented as a sum of contributions independent of and proportional to the Fermi level, respectively:

$$S^{(0)} = -\int \frac{d^3k}{(2\pi)^3}\frac{v_F^2 k_\perp^2}{8E^3}\left\{(3g_p - g_s)^2 b_z^2 + g_s^2 b_\perp^2\right\} - \frac{\mu^2}{8\pi^2 v_F^2 v_z}\left\{(3g_p + g_s)^2 b_z^2 + g_s^2 b_\perp^2\right\}. \tag{10}$$

We note that we have obtained the last row of this equation in the limit of small Fermi level, i.e., when we can view dispersion within each Dirac cone as linear in all directions.

If we assume that the magnetic factors $g_{s,p}$ are close to each other, $g_s \approx g_p$, we can conclude that the coefficient in front of b_z^2 has larger magnitude than the contribution to $b_\perp^2$, and thus magnetic susceptibility will be larger in the z direction. Also, we can notice that, as the chemical potential increases, susceptibility always gets enhanced. This result is different from the type-II Dirac semimetal, the susceptibility of which in one direction does not depend on the the magnitude of the chemical potential. However, it is worth pointing out a special case $g_s = \pm 3g_p$, which could, in principle, happen if the bands did not have orbital momentum and their pseudospin σ or τ were a physical spin. Indeed, in such a case, the terms in Eq. (10) proportional to b_z become trivial, and thus the magnetic susceptibility becomes independent of the chemical potential.

Now, let us explore spatial modulation of the spontaneous magnetization. In the same way as in Sec. II A, we compute quadratic over external momentum q corrections to the effective action and obtain the following expression:

$$\begin{aligned} S^{(2)} = &-\int_{|m|>\mu} dk_z \frac{g_s g_p v_F^2 q_\perp^2 b_z^2}{4v_F^2|m|} \\ &-\int_{|m|>\mu} dk_z \frac{m'^2 q_z^2}{48 v_F^2|m|}\left[(3g_p + g_s)^2 b_z^2 + g_s^2 b_\perp^2\right] \\ &+\int_{|m|>\mu} dk_z \frac{m m'' q_z^2}{32 v_F^2|m|}\left[(3g_p - g_s)^2 b_z^2 + g_s^2 b_\perp^2\right] \\ &+\frac{\pi v_F^2 q_\perp^2}{v_F^2 v_z}\left[\frac{3g_p^2 b_z^2}{2} + \frac{g_s^2 b^2}{3} - \frac{59 g_s g_p b_z^2}{10}\right] \\ &+\frac{\pi}{v_F^2 v_z}\frac{v_z^2 q_z^2}{12}\left[(3g_p - g_s)^2 b_z^2 + g_s^2 b_\perp^2\right]. \end{aligned}$$

We can see that, similarly to the type-II Dirac semimetal, $S^{(2)}$ contains a momentum integral, which diverges in the limit of zero μ, and thus becomes dominant if μ is small (strictly speaking, this divergence appears due to expansion in q; it does not appear when we evaluate Eq. (5) numerically). However, as μ grows, its contribution decreases, whereas the other (i.e., intraband) contribution remains invariant. Thus, we can infer that the z component of the magnetic field is spatially modulated in both the z and the perpendicular direction, but it can undergo crossovers, as μ is increased. Similarly, the perpendicular magnetization $b_\perp$, if present, is spatially modulated in the z direction, and again, with increasing μ, it can undergo crossover. In the Appendix A 1 we present numerical results (see Fig. 2) obtained from lattice regularization of the Hamiltonian (9), which confirm our analytical calculation and also demonstrate that at small μ the spatially modulated magnetic state is antiferromagnetic, but as μ increases it may undergo transition to a spin-density wave state.

Overall, we have found that Dirac semimetals naturally host spatially modulated magnetic ground states, though their specific configurations may depend on details of the model. Furthermore, we have found that the ground state is determined by the competition between the bulk of the Brillouin zone and the Fermi surface, and therefore can change with Fermi level. In the Appendix we consider the same problem numerically on a lattice and obtain that in most cases the ground state is antiferromagnetic, though it can also undergo transitions to a spin-density wave or a ferromagnet.

III. MAGNETIC SUSCEPTIBILITY AT FINITE TEMPERATURES

In the previous section, we studied possible magnetic instabilities in Dirac semimetals at zero temperature and found that spontaneous magnetization occurs at finite wave vector, thus forming an antiferromagnetic or a spin-density wave phase. Now we would like to get an idea of how it may possibly change, once the temperature becomes finite. Since at both finite temperature and wave vector the effective action cannot be computed analytically, we limit our analysis to the case of zero wave vector.

We start from Eq. (6). Since we are only interested in the change of the effective action due to small temperature $T \ll \mu$, we leave only terms which contain $n_F(d-\mu)$ or its first

derivative. After taking the limit $q \to 0$, we obtain

$$\Delta S_2^{(0)} = \int \frac{d^3k}{(2\pi)^3}\left\{\frac{\mathrm{tr}M^2}{2}\left(\frac{n_F(d-\mu)}{2d}+\frac{1}{2}\frac{\partial n_F(d-\mu)}{\partial d}\right)+\frac{\mathrm{tr}(\vec{d}_k\vec{\Gamma})M(\vec{d}_k\vec{\Gamma})M}{2}\left(-\frac{n_F(d-\mu)}{2d^3}+\frac{1}{2d^2}\frac{\partial n_F(d-\mu)}{\partial d}\right)\right\}. \tag{11}$$

For each of the models, we can substitute explicit expressions for the traces, and then take the momentum integrals (see, e.g., Ref. [62] for details of computing integrals over Fermi distributions). However, we also have to account for the fact that μ is a function of temperature. This T dependence (at $T \ll \mu$) can be explicitly found by imposing the condition of conserved particle number $N(T) = \text{const}$ and computing it explicitly:

$$N_{\text{per node}} = \int \frac{d^3k}{(2\pi)^3} n_F(k-\mu) \approx \frac{\mu^3+\pi^2T^2\mu}{6\pi^2},$$

which in turn leads to the following expansion for the chemical potential:

$$\mu \approx E_F - \frac{\pi^2T^2}{3E_F}.$$

Note that the expression for μ does not depend on the number of Weyl nodes.

We can evaluate the effective action (11) by using explicit expressions for the traces, taking momentum integrals and using the above expansion for μ. In the case of a type-II Dirac semimetal, we obtain the following answer:

$$\Delta S_2^{(0)} = -\frac{b_\perp^2 E_F^2}{2\pi^2 v_x v_y v_z} + \frac{b_\perp^2 T^2}{6 v_x v_y v_z}.$$

The most important feature of this expression is that it does not contain any dependency on b_z. In other words, we have obtained a surprising result, that in the leading order, paramagnetic susceptibility $\chi_{ij} = -\frac{\partial^2 \Delta S_2^{(0)}}{\partial b_i \partial b_j}$ of a type-II Dirac semimetal in the z direction is temperature independent. This is the consequence of the fact that, in Dirac semimetals, bands are very close to each other, which makes interband contribution to the susceptibility (Van Vleck paramagnetism) comparable to the intraband contribution (Pauli paramagnetism). Moreover, we were assuming here that the dispersion is linear, which is just an approximation in real materials. However, since we obtained that the susceptibility is temperature independent, it seems that by slight perturbing it is possible to make it either decreasing or increasing with temperature.

In a type-I Dirac semimetal, the answer for the effective action has the form

$$\Delta S_2^{(0)} = -\frac{1}{8\pi^2 v_\perp^2 v_z}\left\{(3g_p+g_s)^2 b_z^2 + g_s^2 b_\perp^2\right\}\left(E_F^2 - \frac{\pi^2T^2}{3}\right).$$

As we can see, the susceptibility is temperature dependent in all directions. However, we note that it becomes temperature independent in the z direction in the special case $g_s = -3g_p$, which could, in principle, happen if the band pseudospin were the same as physical spin.

To summarize our results, we have studied magnetic susceptibility of Dirac semimetals as a function of temperature and found that, in certain cases (namely, when pseudospin coincides with physical spin), it may be temperature independent. In this section, we did not study the behavior of the antiferromagnetic or spin-density wave instabilities at finite temperature, but we consider it numerically in the Appendix A 2 (see Figs. 3, 4 for the cases of type II and I Dirac semimetals respectively). We obtain that the ground state evolves, and, in principle, it may undergo a transition, e.g., from spin-density wave to antiferromagnetic phase.

IV. DISCUSSION

In this paper, we have explored a possibility of spontaneous magnetization in Dirac semimetals, and found that they naturally host antiferromagnetic or spin-density wave ground states. We have also found that their specific structure may vary depending on a particular type of Dirac semimetal, as well as its Fermi energy, temperature, and nonlinear corrections to the Dirac spectrum. However, in special cases, when the bands do not have orbital momentum, magnetic properties of Dirac semimetals, including magnetic susceptibility, may be Fermi energy and temperature independent.

The main reason which makes Dirac semimetals different from other solids lies in the fact that, in contrast to conventional Fermi liquid, magnetization in Dirac semimetals is created not only by electrons on the Fermi surface, but also by electrons from the whole Brillouin zone. In the limit of small chemical potential, i.e., when the Fermi level is close to the Dirac points, the Fermi surface gets reduced to a point or points, and thus the magnetization is created mainly by the bulk of the Brillouin zone. On the other hand, at finite Fermi level, the magnetization arises from competition between the bulk and the Fermi-surface contribution, which results in a possibility of phase transitions with varying Fermi energies.

We expect that our findings may have a lot of implications. In fact, the problem of spatially inhomogeneous magnetization in Weyl/Dirac semimetals has also been extensively studied [63–65], and it was found that it may lead to unusual properties. For example, in the presence of periodic magnetization, there appear novel electronic states, so-called pseudo-Landau levels, which have dispersion forming an "open nodal line." We suggest that such effects may arise due to spin-density waves in Dirac semimetals, which we study in this paper.

We note that a type-II Dirac cone has been experimentally observed in the material $ZrTe_5$ [17]. In fact, this material has been studied for a long time [66]. First, it was discovered as a material which exhibits anomalous resistivity peak at $T = 150$ K [66], but, soon after, it was claimed that such an anomaly is not attributed to a spin- or charge-density wave [67]. We suggest that such a conclusion may be reconsidered, for example, because in the work [67] it was implicitly assumed that the spin- or charge-density wave leads to suppression of carrier densities at Fermi level, but it may not be the case (e.g., if there appear gapless pseudo-Landau levels).

We mention that, in recent years, antiferromagnetism was found to be common in Dirac and Weyl semimetals. A large number of materials where antiferromagnetism coexists with Dirac electrons were discovered. These materials include, for

example, antiferromagnetic NdSb [48,49], where localized spins form ferromagnetic planes which are antiferromagnetically aligned in one of the directions—similarly to the models considered in this paper. Weyl points were also theoretically predicted in antiferromagnets Mg_3Sn and Mg_3Ge [68,69]. More interestingly, in Ref. [45] it was claimed that Dirac electrons enhance antiferromagnetic exchange interaction in the experimentally discovered Dirac semimetals $CaMnBi_2$ and $SrMnBi_2$. Another example of a Weyl semimetal which contains ferromagnetic planes aligned antiferromagnetically is $BaMnSb_2$ [70]. Perhaps, the most interesting material where Dirac electrons coexist with antiferromagnetism is CuMnAs [40,41]: in this material, phase transition between commensurate and incommensurate antiferromagnetism has been observed as a function of temperature and chemical composition (i.e., chemical potential) [40]. Similarly, the material $EuCd_2As_2$ [50] has been predicted to be antiferromagnetic, but it may undergo a transition into a ferromagnetic phase under doping. Finally, we mention Dirac material $Sr_{1-y}Mn_{1-z}Sb_2$ [71], which exhibits so-called canted antiferromagnetic order, i.e., two spin components are antiferromagnetically ordered in such a way that the net magnetization is nonzero, but at higher temperatures it undergoes transition to a ferromagnetic phase. Interplay between antiferromagnetism and Dirac electrons is currently being actively studied, and it leads to novel effects, which have promising applications in spintronics [54].

Here we have presented a simple mean-field picture, explaining why antiferromagnetism naturally appears in Dirac semimetals. We remark that our approach is not to be viewed as rigorous: the mean field is just a rough approximation, which does not always predict quantities (e.g., temperature dependencies) accurately. A significant contribution to the magnetization behavior may arise due to quantum corrections (e.g., magnons), the full electronic structure, etc. In addition, rigorously speaking, magnetic instabilities in Dirac semimetals have to be compared with various instabilities of different types (see e.g., Ref. [72]). Nevertheless, we have demonstrated that the simple mean-field picture successfully explains the origin of antiferromagnetism in Dirac semimetals.

In the future, it might be interesting to derive the same results using more rigorous techniques, e.g., renormalization-group analysis. Finally, we note that while preparing this paper we became aware of an experimental work [73], where charge-density waves were found in closely related Weyl semimetals. We believe that they may be described using the same method as spin-density waves considered in the present paper.

ACKNOWLEDGMENTS

The author would like to thank Anton Burkov for numerous discussions about this work. The author also would like to thank Sergey Syzranov, Susanne Stemmer, Taylor Hughes, Adam Kaminski, and Yun Wu for making useful suggestions and feedback about the project. The work was supported by Natural Sciences and Engineering Research Council of Canada.

APPENDIX: NUMERICAL CALCULATION OF POSSIBLE MAGNETIC GROUND STATES IN DIRAC SEMIMETAL

In this Appendix, we consider lattice versions of the models of type-II and -I Dirac semimetals introduced in the main text, and compute their effective actions [Eq. (5)] numerically. In this way, we are able to find the momentum q of the magnetic ground state [determined by a minimum of the effective action $S(q)$] and its behavior at different μ and T, including the range, when nonlinear corrections to the dispersion become important. We obtain that, typically, at small μ, the momentum q has one of the components equal to π, which tells us that the ground state is antiferromagnetic, whereas at sufficiently large μ (when nonlinear corrections become important) q starts decreasing, thus showing a phase transition from antiferromagnetic to spin-density wave ground state. We note that, throughout our analysis, we do not consider the full 3D range of momenta, which would be computationally challenging, but instead we limit ourselves with just a few special directions of q, which is sufficient for our illustrative purposes.

This section is organized as follows. In Sec. 1 we describe our method of finding the magnetic ground state at zero temperature by considering the model of a type-II Dirac semimetal, and then repeating the calculations for the case of a type-I Dirac semimetal. After this, in Sec. 2 we generalize our method in the case of finite temperatures.

1. Magnetic ground states

Let us describe our approach of finding the magnetic ground states by using an example of a type-II Dirac semimetal. We replace the coefficients d_i from Eq. (2) with their lattice counterparts, which, in the type-II case, have the form

$$d_2 = v_z \sin k_z, \qquad d_3 = v_y \sin k_y, \qquad d_4 = v_x \sin k_x. \tag{A1}$$

We use these expressions to compute numerically the effective action [see Eq. (6)]. More specifically, we evaluate the momentum integral entering the effective action (6) over the Brillouin zone (i.e., over the range $-\pi < k_{x,y,z} < \pi$) by using the tetrahedral method [74]. Its main idea is that after the integration range is split into cubes by discretizing momentum each of the cubes is additionally split into nine tetrahedra. This approach helps us resolve issues, which may happen due to divergences near the Fermi surface in the numerator and denominator of Eq. (6). We present our findings in Fig. 1. One can see that for some directions of the momentum q_i the effective action has a minimum at zero q_i, as was predicted by Eq. (8), whereas for others the minimum is reached at finite values of q_i. For example, in the case of $b \parallel x$ [see Fig. 1(a)], the effective action increases with q_x, and the curvature decreases with increasing μ consistently with Eq. (8). At the same time, the effective action describing b_x as a function of $q_{y,z}$ [see Fig. 1(b)] has a minimum away from zero. Thus, the b_x component of the magnetization is spatially modulated both in y and z directions.

In a similar way, one can see that magnetization b_z [see Fig. 1(c)] is spatially modulated in the z direction (as we will see, this is due to nonlinear corrections to the energy spectrum). At small values of the chemical potential μ, the

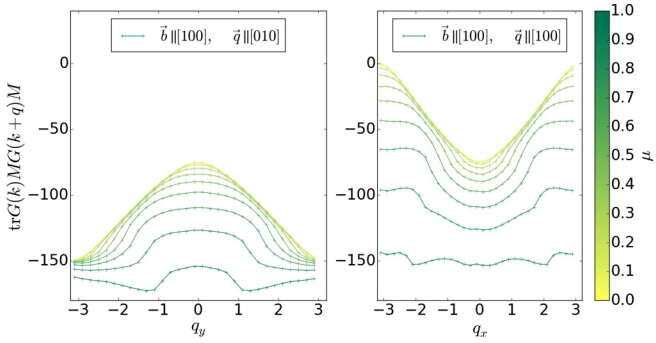

(a) $\vec{b} \parallel \vec{x}$

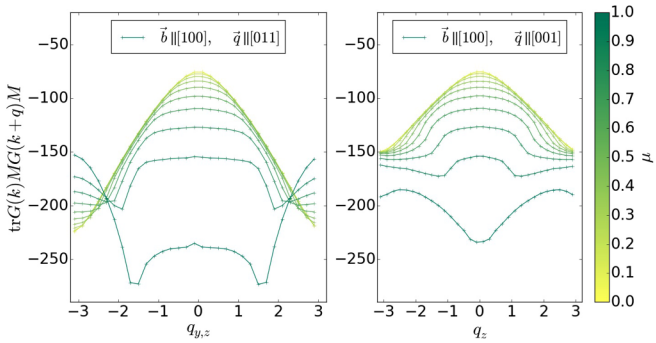

(b) $\vec{b} \parallel \vec{x}$

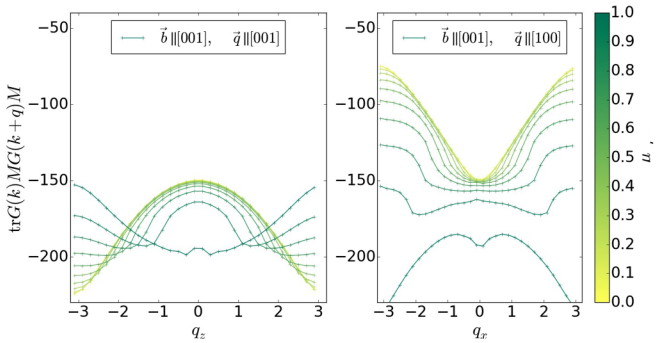

(c) $\vec{b} \parallel \vec{z}$

FIG. 1. Numerically computed effective action (5) for a type-II Dirac semimetal placed on a lattice [Eqs. (1) and (A1)] as a function of external momentum q for different values of the chemical potential μ. The directions of the magnetization b and momentum q are (a) $\vec{b} = (0.5, 0, 0)$ and $\vec{q} = (0, q_y, 0)$, $\vec{q} = (q_x, 0, 0)$; (b) $\vec{b} = (0.5, 0, 0)$ and $q = q_y = q_z$, $\vec{q} = (0, 0, q_z)$; and (c) $\vec{b} = (0, 0, 0.5)$ and $\vec{q} = (0, 0, q_z)$, $\vec{q} = (q_x, 0, 0)$. At small chemical potential μ, the magnetization component b_x is modulated in the y direction, whereas b_z is modulated in the z direction, but at $\mu = 1.0$ a phase transition occurs: the modulation of b_z changes from the z to the x direction.

effective action has a minimum at the boundary of the Brillouin zone, which implies that the ground state is antiferromagnetic. However, at larger values of μ, spatial modulation of the ground state decreases, so that it starts forming a spin-density wave. Eventually, spatial modulation in the z direction disappears, but, on the other hand, it appears in the x direction. Thus, as μ increases, there appears a phase transition between two spin-density waves modulated in different directions.

We note that our numerical results have minor deviations from the analytical ones, but the difference is explained by

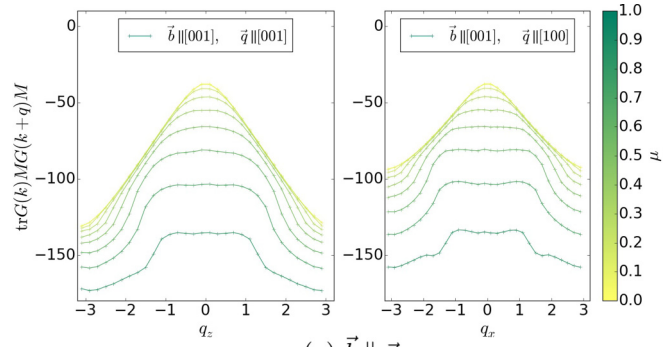

(a) $\vec{b} \parallel \vec{z}$

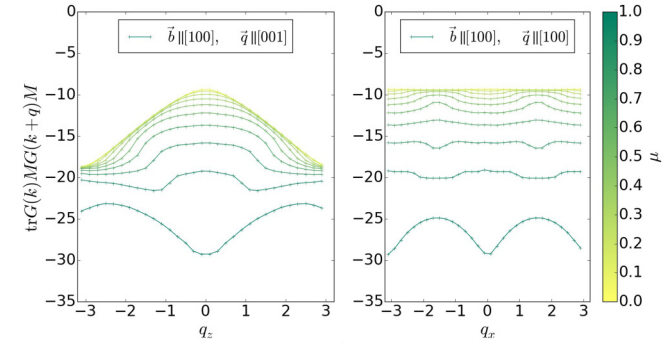

(b) $\vec{b} \parallel \vec{x}$

FIG. 2. Numerically computed effective action (5) for a type-I Dirac semimetal [Eqs. (9) and (A2)] as a function of q_z, q_x for various values of the chemical potential μ. The parameters of the model are $m_0 = 1.0$, $m_1 = 1.0$, $g_s = g_p = 1.0$. The magnetic field is (a) $\vec{b} = (0, 0, 0.5)$ and (b) $\vec{b} = (0.5, 0, 0)$. At small values of μ, the magnetization $b_{x,z}$ has minima at either $p_x = \pi$ or $p_z = \pi$. However, at large μ, the local minimum gets displaced away from the boundary of the Brillouin zone. Thus, at small μ, the magnetization $b_{x,z}$ forms an antiferromagnetic configuration, but with increasing μ it changes into a spin-density wave.

the nonlinearity of dispersion. For example, from Eq. (8) we expect that, in the case of strictly linear dispersion, the term $q_z^2 b_z^2$ should have zero bulk contribution and small positive contribution from the Fermi surface. However, since on a lattice the dispersion (A1) is nonlinear, it has indeed a large negative bulk contribution responsible for the shape of the curves in Fig. 1(c). Similarly, the wavelength of spin-density waves is determined by scales of the band. In realistic materials, we expect nonlinear corrections to play a weaker role than in our simulations, since their scale is much larger than the chemical potential, but our main conclusion is that nonlinear corrections to the band structure may change magnetic ground states in numerous ways, even though they are still expected to be spatially modulated.

Now, let us repeat the calculations in the case of a type-I Dirac semimetal. In a similar way, we compute the effective action (6) for the model (9) placed on a lattice. We choose the functions d as

$$\begin{aligned} d_1 &= \sin k_x, \\ d_2 &= \sin k_y, \\ d_3 &= m_0 - m_1(1 - \cos k_z). \end{aligned} \tag{A2}$$

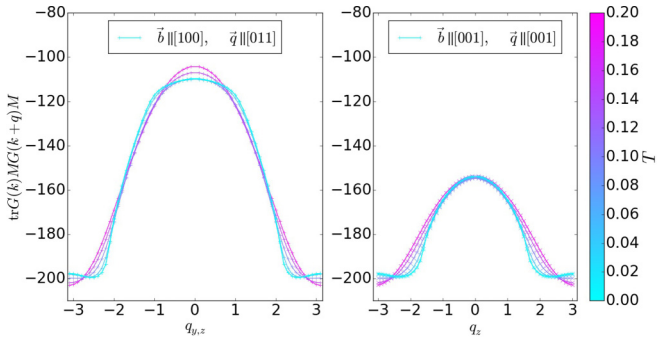

FIG. 3. Numerically computed effective action (5) for a type-II Dirac semimetal [Eq. (A1)] at various temperatures. The magnetic field and momentum have the directions $b = (b_x, 0, 0)$, $q = (0, q, q)$ (left) and $b = (0, 0, b_z)$, $q = (0, 0, q_z)$ (right). The Fermi level is $E_F = 0.7$, and the other parameters are the same as in Fig. 1. At zero T, the minimum of the effective action is away from the boundary of the Brillouin zone, but approaches it as T increases. Thus the system undergoes a phase transition from antiferromagnetic to spin-density wave phase.

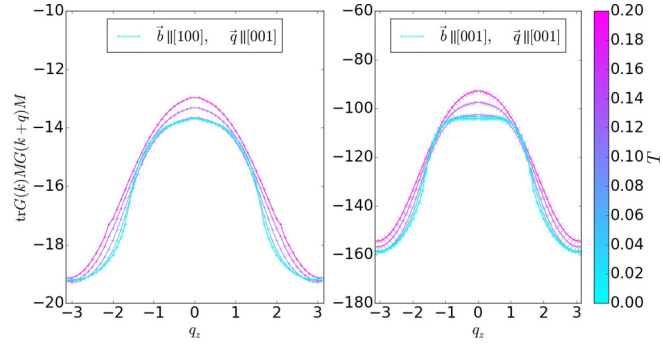

FIG. 4. Numerically computed effective action for a type-I Dirac semimetal [Eq. (A2)] at various temperatures. Here $b = (b_x, 0, 0)$, $q = (0, 0, q_z)$ (left) and $b = (0, 0, b_z)$, $q = (0, 0, q_z)$ (right). The Fermi level is $\mu = 0.7$, and the other parameters are the same as in Fig. 2.

We present our findings in Fig. 2(b). One can see that in the case of magnetization in the z direction the effective action has local minima either at X or at the Z point of the Brillouin zone, i.e., at $q = (\pi, 0, 0)$ or $(0, 0, \pi)$, which suggest that b_z can be spatially modulated in both x and z directions. On the other hand, b_x is modulated in the z direction: at small μ, it forms an antiferromagnet, but, as μ increases, a transition to the spin-density wave phase occurs. Eventually, at large μ, a phase transition occurs: spatial modulation in the z direction disappears, and the system becomes spatially modulated in the x direction.

2. Magnetic ground states at finite temperatures

Once we found the magnetic ground states at zero temperature, we can try to study their evolution, once temperature becomes finite. Specifically, we would like to compute numerically the effective action (6) at finite temperatures. Since n_F and its derivative significantly deviate from constant only in a narrow range of parameters, straightforward tetrahedral integration is challenging. For this reason, to obtain the effective action at finite temperature, we first compute it for various chemical potentials at zero temperature, and then obtain the answer at finite temperatures by applying a discretized version of the following relation [75]:

$$S(T, \mu) = -\int d\xi \frac{\partial n_F(\xi - \mu)}{\partial \xi} S(0, \xi). \tag{A3}$$

In addition, we have to account explicitly for the change of chemical potential with temperature, which we do in the following way. First, we numerically compute particle number at zero temperature as a function of chemical potential: $N = \int \frac{d^3k}{(2\pi)^3}\theta(\mu - k)$. Then, by using Eq. (A3), we obtain particle number $N(\mu, T)$ at various finite temperatures and chemical potentials and use it to find the dependency $\mu(T)$. Namely, for a given chemical potential at zero temperature E_F, we take number of particles $N(E_F, T = 0)$; then, for given nonzero T, find two closest values of $N(T)$ and their corresponding μ and finally obtain the answer for $\mu(T)$ through their linear interpolation. In total, we find $\mu(T)$ for given E_F and then use it to compute the effective action through Eq. (A3).

In the case of a type-II Dirac semimetal, we present our findings in Fig. 3. At $q = 0$ we expect that the effective action will be temperature independent for $b \parallel z$, but will increase, e.g., for $b \parallel x$. Our numerical plots are consistent with these predictions at small T, but as T becomes large the numerical plots start behaving differently because of nonlinearities in the dispersion. More interestingly, our numerical findings confirm that the wave vector of the magnetization changes with temperature, and, even more, as temperature grows, the system may undergo a phase transition from spin-density wave to antiferromagnetic phase.

The results for the type-I Dirac semimetal are qualitatively similar to the type-II case and are shown in Fig. 4. As expected, the magnitude of the effective action decreases with temperature, and its shape evolves. Specifically, its minimum may shift, so that the system undergoes a transition from spin-density wave to antiferromagnetic phase.

Thus, we have demonstrated that Dirac electrons may have a large variety of possible magnetic phases. Most commonly, these phases are antiferromagnetic or spin-density wave, and there are possible transitions between them, as chemical potential or temperature varies.

[1] N. P. Armitage, E. J. Mele, and A. Vishwanath, Rev. Mod. Phys. **90**, 015001 (2018).

[2] S.-Y. Xu, I. Belopolski, N. Alidoust, M. Neupane, G. Bian, C. Zhang, R. Sankar, G. Chang, G. Yuan, C.-C. Lee, S.-M. Huang, H. Zheng, J. Ma, D. S. Sanchez, B. Wang, A. Bansil, F. Chou, P. P. Shibayev, H. Lin, S. Jia, and M. Z. Hasan, Science **349**, 613 (2015).

[3] X. Wan, A. M. Turner, A. Vishwanath, and S. Y. Savrasov, Phys. Rev. B **83**, 205101 (2011).

[4] A. A. Burkov and L. Balents, Phys. Rev. Lett. **107**, 127205 (2011).

[5] S.-M. Huang, S.-Y. Xu, Belopolski, C.-C. Lee, G. Chang, B. Wang, G. Alidoust, Nasserand Bian, M. Neupane, C. Zhang, S. Jia, A. Bansil, H. Lin, and M. Z. Hasan, Nat. Commun. **6**, 8373 (2015).

[6] L. X. Yang, Z. K. Liu, Y. Sun, H. Peng, H. F. Yang, T. Zhang, B. Zhou, Y. Zhang, Y. F. Guo, M. Rahn *et al.*, Nat. Phys. **11**, 728 (2015).

[7] S.-Y. Xu, I. Belopolski, C. Sanchez, Daniel S. Zhang, G. Chang, C. Guo, G. Bian, Z. Yuan, H. Lu, T.-R. Chang, P. P. Shibayev, M. L. Prokopovych, N. Alidoust, H. Zheng, C.-C. Lee, S.-M. Huang, R. Sankar, F. Chou, C.-H. Hsu, H.-T. Jeng, A. Bansil, T. Neupert, V. N. Strocov, H. Lin, S. Jia, and M. Z. Hasan, Sci. Adv. **1**, e1501092 (2015).

[8] S.-Y. Xu, N. Alidoust, I. Belopolski, Z. Yuan, G. Bian, T.-R. Chang, H. Zheng, V. N. Strocov, D. S. Sanchez, G. Chang, C. Zhang, D. Mou, Y. Wu, L. Huang, C.-C. Lee, S.-M. Huang, B. Wang, A. Bansil, H.-T. Jeng, T. Neupert, A. Kaminski, H. Lin, S. Jia, and M. Z. Hasan, Nat. Phys. **11**, 748 (2015).

[9] G. Volovik, JETP **46**, 401 (1977).

[10] S. M. Young, S. Zaheer, J. C. Y. Teo, C. L. Kane, E. J. Mele, and A. M. Rappe, Phys. Rev. Lett. **108**, 140405 (2012).

[11] Z. Wang, Y. Sun, X.-Q. Chen, C. Franchini, G. Xu, H. Weng, X. Dai, and Z. Fang, Phys. Rev. B **85**, 195320 (2012).

[12] Z. K. Liu, B. Zhou, Y. Zhang, Z. J. Wang, H. M. Weng, D. Prabhakaran, S.-K. Mo, Z. X. Shen, Z. Fang, X. Dai, Z. Hussain, and Y. L. Chen, Science **343**, 864 (2014).

[13] S. Borisenko, Q. Gibson, D. Evtushinsky, V. Zabolotnyy, B. Büchner, and R. J. Cava, Phys. Rev. Lett. **113**, 027603 (2014).

[14] M. Neupane, S.-Y. Xu, R. Sankar, N. Alidoust, G. Bian, C. Liu, I. Belopolski, T.-R. Chang, H.-T. Jeng, H. Lin, A. Bansil, F. Chou, and M. Z. Hasan, Nat. Commun. **5**, 3786 (2014).

[15] Z. K. Liu, J. Jiang, B. Zhou, Z. J. Wang, Y. Zhang, H. M. Weng, D. Prabhakaran, S.-K. Mo, H. Peng, P. Dudin, T. Kim, M. Hoesch, Z. Fang, X. Dai, Z. X. Shen, D. L. Feng, Z. Hussain, and Y. L. Chen, Nat. Mater. **13**, 677 (2014).

[16] R. Y. Chen, Z. G. Chen, X.-Y. Song, J. A. Schneeloch, G. D. Gu, F. Wang, and N. L. Wang, Phys. Rev. Lett. **115**, 176404 (2015).

[17] A. Pariari and P. Mandal, Sci. Rep. **7**, 40327 (2017).

[18] J. Cano, B. Bradlyn, Z. Wang, M. Hirschberger, N. P. Ong, and B. A. Bernevig, Phys. Rev. B **95**, 161306(R) (2017).

[19] A. A. Burkov, Phys. Rev. Lett. **120**, 016603 (2018).

[20] E. Kogan and M. Kaveh, Phys. Status Solidi B **252**, 2789 (2015).

[21] Y. Araki and K. Nomura, Phys. Rev. B **93**, 094438 (2016).

[22] M. V. Hosseini and M. Askari, Phys. Rev. B **92**, 224435 (2015).

[23] H.-R. Chang, J. Zhou, S.-X. Wang, W.-Y. Shan, and D. Xiao, Phys. Rev. B **92**, 241103(R) (2015).

[24] M. Koshino and I. F. Hizbullah, Phys. Rev. B **93**, 045201 (2016).

[25] Y. Ominato and K. Nomura, Phys. Rev. B **97**, 245207 (2018).

[26] G. P. Mikitik and Y. V. Sharlai, Phys. Rev. B **94**, 195123 (2016).

[27] S.-S. Zhang, J. Ye, and W.-M. Liu, Phys. Rev. B **94**, 115121 (2016).

[28] D. A. Abanin and D. A. Pesin, Phys. Rev. Lett. **106**, 136802 (2011).

[29] C.-X. Liu, B. Roy, and J. D. Sau, Phys. Rev. B **94**, 235421 (2016).

[30] M. Shiranzaei, H. Cheraghchi, and F. Parhizgar, Phys. Rev. B **96**, 024413 (2017).

[31] G. Rosenberg and M. Franz, Phys. Rev. B **85**, 195119 (2012).

[32] J. Wang, B. Lian, and S.-C. Zhang, Phys. Rev. Lett. **115**, 036805 (2015).

[33] J. Sun, L. Chen, and H.-Q. Lin, Phys. Rev. B **89**, 115101 (2014).

[34] X.-Q. Sun, S.-C. Zhang, and Z. Wang, Phys. Rev. Lett. **115**, 076802 (2015).

[35] M. Laubach, C. Platt, R. Thomale, T. Neupert, and S. Rachel, Phys. Rev. B **94**, 241102(R) (2016).

[36] M. Trescher, E. J. Bergholtz, M. Udagawa, and J. Knolle, Phys. Rev. B **96**, 201101(R) (2017).

[37] J. Maciejko and R. Nandkishore, Phys. Rev. B **90**, 035126 (2014).

[38] Z. Wang and S.-C. Zhang, Phys. Rev. B **87**, 161107(R) (2013).

[39] Y. Wang and P. Ye, Phys. Rev. B **94**, 075115 (2016).

[40] E. Emmanouilidou, H. Cao, P. Tang, X. Gui, C. Hu, B. Shen, J. Wu, S.-C. Zhang, W. Xie, and N. Ni, Phys. Rev. B **96**, 224405 (2017).

[41] P. Tang, Q. Zhou, G. Xu, and S.-C. Zhang, Nat. Phys. **12**, 1100 (2016).

[42] M. Veis, J. Minár, G. Steciuk, L. Palatinus, C. Rinaldi, M. Cantoni, D. Kriegner, K. K. Tikuišis, J. Hamrle, M. Zahradník, R. Antoš, J. Železny, L. šmejkal, X. Marti, P. Wadley, R. P. Campion, C. Frontera, K. Uhlířová, T. Duchoň, P. Kuže, V. Novák, T. Jungwirth, and K. Výborný, Phys. Rev. B **97**, 125109 (2018).

[43] L. Šmejkal, J. Železný, J. Sinova, and T. Jungwirth, Phys. Rev. Lett. **118**, 106402 (2017).

[44] Y. F. Guo, A. J. Princep, X. Zhang, P. Manuel, D. Khalyavin, I. I. Mazin, Y. G. Shi, and A. T. Boothroyd, Phys. Rev. B **90**, 075120 (2014).

[45] A. Zhang, C. Liu, C. Yi, G. Zhao, T.-l. Xia, J. Ji, Y. Shi, R. Yu, X. Wang, C. Chen, and Q. Zhang, Nat. Commun. **7**, 13833 (2016).

[46] M. Neupane, M. M. Hosen, I. Belopolski, N. Wakeham, K. Dimitri, N. Dhakal, J.-X. Zhu, M. Z. Hasan, E. D. Bauer, and F. Ronning, J. Phys.: Condens. Matter **28**, 23LT02 (2016).

[47] D. Mukamel, J. M. Hastings, L. M. Corliss, and J. Zhuang, Phys. Rev. B **32**, 7367 (1985).

[48] Y. Wang, J. H. Yu, Y. Q. Wang, C. Y. Xi, L. S. Ling, S. L. Zhang, J. R. Wang, Y. M. Xiong, T. Han, H. Han, J. Yang, J. Gong, L. Luo, W. Tong, L. Zhang, Z. Qu, Y. Y. Han, W. K. Zhu, L. Pi, X. G. Wan, C. Zhang, and Y. Zhang, Phys. Rev. B **97**, 115133 (2018).

[49] N. Wakeham, E. D. Bauer, M. Neupane, and F. Ronning, Phys. Rev. B **93**, 205152 (2016).

[50] L.-L. Wang, N. H. Jo, B. Kuthanazhi, Y. Wu, R. J. McQueeney, A. Kaminski, and P. C. Canfield, Phys. Rev. B **99**, 245147 (2019).

[51] P. Wadley, B. Howells, J. Železný, C. Andrews, V. Hills, R. P. Campion, V. Novák, K. Olejník, F. Maccherozzi, S. S. Dhesi, S. Y. Martin, T. Wagner, J. Wunderlich, F. Freimuth, J. Mokrousov, Y. Kuneš, J. S. Chauhan, M. J. Grzybowski, A. W. Rushforth, K. W. Edmonds, B. L. Gallagher, and T. Jungwirth, Science **351**, 587 (2016).

[52] J. Železný, H. Gao, K. Výborný, J. Zemen, J. Mašek, A. Manchon, J. Wunderlich, J. Sinova, and T. Jungwirth, Phys. Rev. Lett. **113**, 157201 (2014).

[53] A. Scholl, M. Liberati, E. Arenholz, H. Ohldag, and J. Stöhr, Phys. Rev. Lett. **92**, 247201 (2004).
[54] L. Smejkal, T. Jungwirth, and J. Sinova, Phys. Status Solidi **11**, 1700044 (2017).
[55] A. Altland and B. Simons, *Condensed Matter Field Theory* (Cambridge University, Cambridge, England, 2010).
[56] E. Fradkin, *Field Theories of Condensed Matter Physics* (Cambridge University, Cambridge, England, 2013).
[57] J. König, H.-H. Lin, and A. H. MacDonald, Phys. Rev. Lett. **84**, 5628 (2000).
[58] T. Dietl, H. Ohno, F. Matsukura, J. Cibert, and D. Ferrand, Science **287**, 1019 (2000).
[59] A. A. Burkov, Phys. Rev. Lett. **113**, 187202 (2014).
[60] G. Bednik, A. A. Zyuzin, and A. A. Burkov, New J. Phys. **18**, 085002 (2016).
[61] S. Lee, Y. Inoue, D. Kim, A. Reuveny, K. Kuribara, T. Yokota, J. Reeder, M. Sekino, T. Sekitani, Y. Abe *et al.*, Nat. Commun. **5**, 5898 (2014).
[62] L. Landau and E. Lifshitz, *Statistical Physics* (Elsevier, Amsterdam, 2013), Vol. 5.
[63] E. Tang and L. Fu, Nat. Phys. **10**, 964 (2014).
[64] A. G. Grushin, J. W. F. Venderbos, A. Vishwanath, and R. Ilan, Phys. Rev. X **6**, 041046 (2016).
[65] Bednik, Grigory, Topological and superconducting properties of Weyl and Dirac metals, Ph.D. thesis, University of Waterloo, 2018.
[66] S. Okada, T. Sambongi, and M. Ido, J. Phys. Soc. Jpn. **49**, 839 (1980).
[67] S. Okada, T. Sambongi, M. Ido, Y. Tazuke, R. Aoki, and O. Fujita, J. Phys. Soc. Jpn. **51**, 460 (1982).
[68] J. Liu and L. Balents, Phys. Rev. Lett. **119**, 087202 (2017).
[69] H. Yang, Y. Sun, Y. Zhang, W.-J. Shi, S. S. P. Parkin, and B. Yan, New J. Phys. **19**, 015008 (2017).
[70] S. Huang, J. Kim, W. A. Shelton, E. W. Plummer, and R. Jin, Proc. Natl. Acad. Sci. USA **114**, 6256 (2017).
[71] J. Y. Liu, J. Hu, Q. Zhang, D. Graf, H. B. Cao, S. M. A. Radmanesh, D. J. Adams, Y. L. Zhu, G. F. Cheng, X. Liu, W. A. Phelan, J. Wei, M. Jaime, F. Balakirev, D. A. Tennant, J. F. DiTusa, I. Chiorescu, Z. Q. Spinu, and L. Mao, Nat. Mater. **16**, 905 (2017).
[72] B. Roy, P. Goswami, and V. Juričić, Phys. Rev. B **95**, 201102(R) (2017).
[73] W. Shi, B. J. Wieder, H. L. Meyerheim, Y. Sun, Y. Zhang, Y. Li, L. Shen, Y. Qi, L. Yang, J. Jena, P. Werner, K. Koepernik, S. Parkin, Y. Chen, C. Felser, B. A. Bernevig, and Z. Wang, arXiv:1909.04037.
[74] J. Rath and A. J. Freeman, Phys. Rev. B **11**, 2109 (1975).
[75] P. E. Blöchl, O. Jepsen, and O. K. Andersen, Phys. Rev. B **49**, 16223 (1994).